Running head: Python toolbox for silent substitution

PySilSub: An open-source Python toolbox for implementing the method of silent substitution

in vision and non-visual photoreception research

Joel T. Martin[1], Geoffrey M. Boynton[2], Daniel H. Baker[1,3], Alex R. Wade[1,3] and Manuel Spitschan[4,5,6]

[1]Department of Psychology, University of York, York, United Kingdom

[2]Department of Psychology, University of Washington, Seattle, WA

[3]York Biomedical Research Institute, University of York, York, United Kingdom

[4]Max Planck Institute for Biological Cybernetics, Tübingen, Germany

[5]TUM Department of Sport and Health Sciences (TUM SG), Technical University of Munich, Munich, Germany

[6]TUM Institute for Advanced Study (TUM-IAS), Technical University of Munich, Garching, Germany

Author Note

Address: Joel T. Martin, Department of Psychology, University of York, York, United Kingdom, YO10 5DD

Phone: +44 (0)1904 323190

Email: joel.martin@york.ac.uk

PYTHON TOOLBOX FOR SILENT SUBSTITUTION

Abstract

The normal human retina contains several classes of photosensitive cell—rods for low-light vision, three cone classes for daylight vision, and the intrinsically photosensitive retinal ganglion cells (ipRGCs) expressing melanopsin for non-image-forming functions including pupil size, melatonin suppression and circadian photoentrainment. The spectral sensitivities of the photoreceptors overlap significantly, which means that most lights will stimulate all photoreceptors, to varying degrees. The method of silent substitution is a powerful tool for stimulating individual photoreceptor classes selectively, which is useful in research and clinical settings. The main hardware requirement for silent substitution is a spectrally calibrated light stimulation system with at least as many primaries as there are photoreceptors under consideration. Device settings that will produce lights to selectively stimulate the photoreceptor(s) of interest can be found using a variety of analytic and algorithmic approaches. Here we present *PySilSub* (https://github.com/PySilentSubstitution/pysilsub), a novel Python package for silent substitution featuring flexible object-oriented support for individual colorimetric observer models (including human and mouse observers), multi-primary stimulation devices, and solving silent substitution problems with linear algebra and constrained numerical optimisation. The software is registered with the Python Package Index and includes example data sets from various multi-primary systems. We hope that *PySilSub* will facilitate the application of silent substitution in research and clinical settings.

Keywords: silent substitution, melanopsin, cones, rods, photoreceptors, instrumentation, pupillary light reflex, software, open source, Python

PySilSub: An open-source Python package for implementing the method of silent

substitution in vision and non-visual photoreception research

The normal human retina contains several types of photosensitive cell (for review, see Grünert & Martin, 2020). Enabling colour and spatial vision at mesopic and photopic light levels are the short- (S), medium- (M), and long- (M) wavelength-light-sensitive cones. Cone cells are packed densely into the fovea and distributed more sparsely elsewhere. Spatial vision at scotopic light levels is mediated by the rods. Though absent from the fovea, rods are the most numerous of the photoreceptor cells and are otherwise widely distributed across the retina. Finally, the intrinsically photosensitive retinal ganglion cells (ipRGCs) express the photopigment melanopsin in their axons and soma (Provencio et al., 2000) and provide an additional light-sensing pathway. ipRGCs do not contribute to vision in the same way as rods and cones but they do play important roles in "non-visual" function, including circadian photoentrainment and control of pupil size, via direct projections to the suprachiasmatic nucleus of the hypothalamus and the olivary pretectal nucleus of the midbrain, respectively (Gamlin et al., 2007; Ruby et al., 2002).

As illustrated in Figure 1, the photoreceptor classes have different spectral sensitivities. The curve for each type of photoreceptor describes the probability of its capturing a photon at a given wavelength, so S cones are about 10 times more likely than L-cones to capture photons at 450 nm, and the likelihood of L and M cones capturing at 550 nm is roughly the same. Because the spectral sensitivities of the photoreceptors overlap, most lights in the visible spectrum will stimulate all types of photoreceptor, albeit to varying degrees. However, it is possible to prepare light stimuli that selectively target photoreceptor classes via the method of silent substitution (Estévez & Spekreijse, 1982).
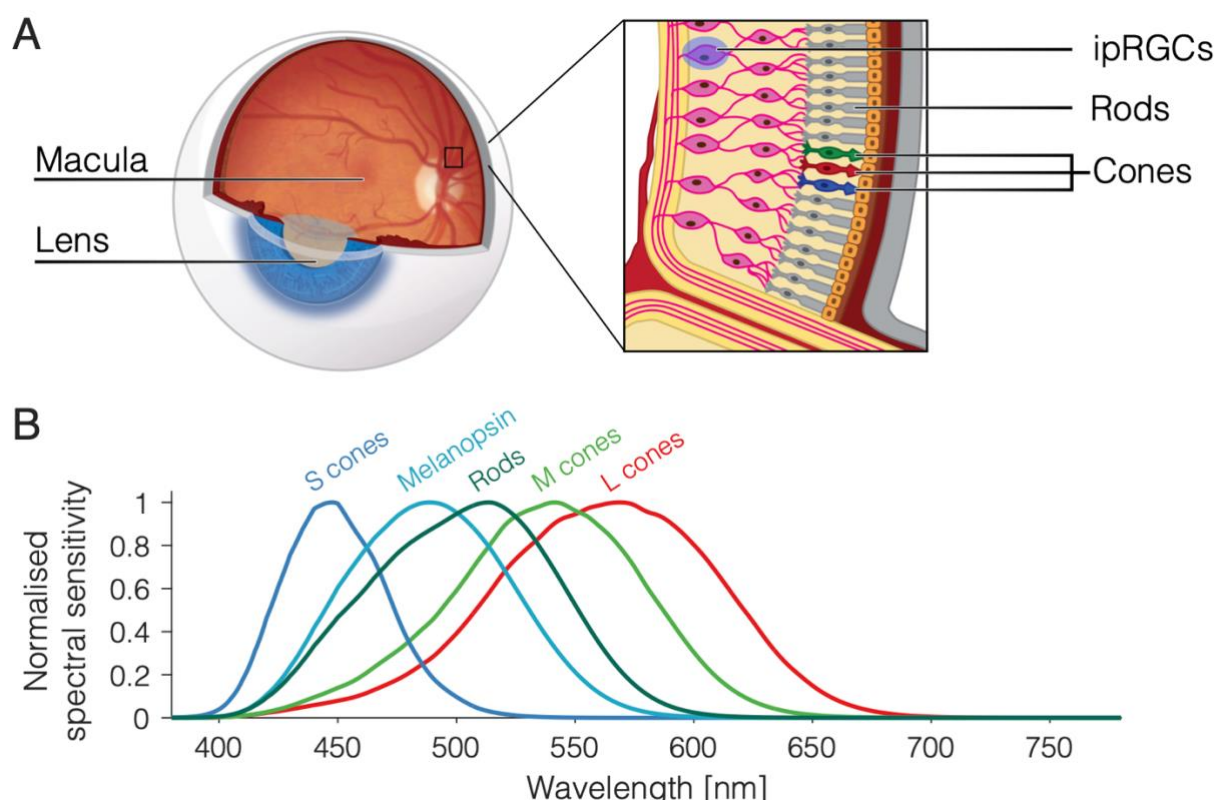
Figure 1. Photoreceptors and their spectral sensitivities (adapted from Figure 3 of Blume et al., 2019; reproduced under the CC BY 4.0 license, http://creativecommons.org/licenses/by/4.0/). (A) Human eye with inset showing the three types of retinal photoreceptor: rods, cones, and intrinsically photosensitive retinal ganglion cells (ipRGCs). (B) Overlapping spectral sensitivities of retinal photoreceptors. The curve for each photoreceptor describes the relative probability of photon capture at a given wavelength.

Silent substitution is an elegant technique that involves using a spectrally calibrated multiprimary stimulation system to produce spectra that selectively stimulate one class of retinal photoreceptor whilst maintaining a constant level of activation in the others. The method exploits Rushton's (1972) principle of univariance, which states that the output of a photoreceptor is one-dimensional and depends upon quantum catch, not upon which quanta are caught. In other words, different spectra will have an identical effect on a photoreceptor providing they lead to the same number of photons being absorbed. The principle of univariance and its relevance to silent substitution is covered in greater detail by Estévez and Spekreijse (1982), along with a treatment of the method's history. In vision science, silent substitution has contributed to our understanding of human colour vision mechanisms (Horiguchi et al., 2013) and it has enabled researchers to examine how targeted

photoreceptor stimulation affects physiological responses such as the electroretinogram (Maguire et al., 2017), and the pupillary light reflex (Spitschan et al., 2014). The method of silent substitution can be used to generate metamers: spectra that have different wavelength distributions but which produce the same cone excitation (the principle underlying all modern colour display devices). Such lights can be used to stimulate pathways contributing to "non-visual" responses to light, including melatonin suppression (Allen et al., 2018; Blume et al., 2022; Souman et al., 2018), sleep (Blume et al., 2022; Schöllhorn et al., 2023), and other neuroendocrine and circadian functions (Zandi et al., 2021). The method of silent substitution can also be used to investigate the contribution of melanopsin signaling to canonical visual processing (Allen et al., 2019; Brown et al., 2012; DeLawyer et al., 2020; Spitschan et al., 2017; Uprety et al., 2022; Vincent et al., 2021), and its potential as a diagnostic tool for retinal disease has garnered attention in recent years (Kuze et al., 2017; Wise et al., 2021).

The main hardware requirement for silent substitution is a spectrally calibrated stimulation system with at least as many primaries as there are photoreceptors of interest. With three cone classes in addition to rods and ipRGCs, this generally means that five primaries are needed, although four may suffice when working in the photopic range as rods become saturated and incapable of signaling above 300 cd/m^2 (Adelson, 1982; Aguilar & Stiles, 1954; but see Kremers et al., 2009; Shapiro, 2002; Sharpe et al., 1989). The primaries should be independently addressable, additive, and ideally stable over time with a linear input-output function. Peak wavelength and bandwidth of the primaries are key considerations that will define the gamut and available contrast (Evéquoz et al., 2021), and the light source needs to be integrated into an optical setup for stimulus delivery (Barrionuevo et al, 2022)—usually Ganzfeld (e.g., Martin et al., 2021; Geisser et al., 2019), specialised Maxwellian view (e.g., Cao et al., 2015; Nugent & Zele, 2022), projector (Allen et al., 2018; Allen et al., 2019; DeLawyer et al., 2020; Hexley et al., 2020; Spitschan et al., 2019; Yamakawa et al., 2019) or display (Blume et al., 2022; Schöllhorn et al., 2023) systems. In a review on stimulation devices used in the literature, Conus and Geiser (2020)

PYTHON TOOLBOX FOR SILENT SUBSTITUTION

found that in most cases the device had 4 or 5 primaries and was built from scratch using LEDs, optical bench components, and microprocessors (e.g., Arduino) with intensity controlled by pulse width modulation.

Also required for silent substitution are estimates of the photoreceptor action spectra of the observer, which, in humans, vary even among colour-normal observers due to differences in ocular physiology. Before striking the retina, incident light must first travel through the lens and ocular media pigment of the observer, which act as prereceptoral filters to effectively shift the spectral sensitivity of the underlying photoreceptors. The crystalline lens of the eye accumulates its yellow pigment with age due to absorption of near-UV radiation (Norren & Vos, 1974; Pokorny et al., 1987; Weale, 1988) and a yellower lens transmits less short-wavelength light. The macula pigment is a yellow carotenoid spot that sits above foveal photoreceptors and reduces the spectral sensitivity of underlying cones in a manner that becomes more pronounced for smaller stimulus field sizes (Chen et al., 2001; Whitehead et al., 2006). Observer age and stimulus field size therefore combine to alter the effective spectral sensitivity functions of a given observer under particular viewing conditions (Figure 2; see also Figure 5, A-B).
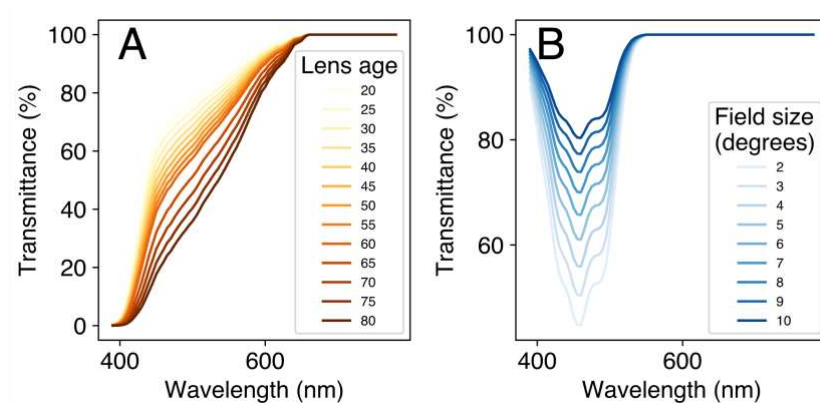

Figure 2. Prereceptoral filtering of light by ocular media. Spectral transmittance functions of (A) the human lens for ages 20 to 80 years (older lenses transmit less light), and (B) the macula pigment for field sizes 2° to 10°. The human lens naturally accumulates a yellow pigment with age due to absorption of near-UV radiation (Lerman, 1980; Feldman et al., 2022) and the macula pigment is a yellow carotenoid spot at the position of the fovea (see Grünert & Martin, 2020, Fig 1). All transmittance functions were calculated in accordance with CIEPO06 (CIE, 2006).

PYTHON TOOLBOX FOR SILENT SUBSTITUTION

The International Commission on Illumination (CIE) defines average colorimetric observer models with estimates of photoreceptor spectral sensitivities for a given age and field size. The CIE observers are based on decades of research involving predominantly psychophysical methods (Smith & Pokorny, 1975; Stiles & Burch, 1959; Stockman et al., 1993, 1999; Stockman & Sharpe, 2000; Vos & Walraven, 1970) but also techniques such as suction electrode recording and microspectrophotometry of photoreceptors (e.g., Baylor et al., 1984; Bowmaker et al., 1978; Bowmaker & Dartnall, 1980). The CIE 2006 Physiological Observer (developed in CIE 170-1:2006 and abbreviated here as CIEPO06: CIE, 2006) defines fundamental cone spectral sensitivity functions for 2° and 10° field sizes and outlines a framework for calculating average spectral sensitivity functions for any age between 20 and 80 years and any field size between 1° and 10°. More recently, prompted by the pioneering research into melanopsin-containing ipRGCs (e.g., Al Enezi et al., 2011; Berson et al., 2002; Brown et al., 2013; Dacey et al., 2005; Gamlin et al., 2007; Lucas et al., 2014; Provencio et al., 2000; Spitschan, 2019), the CIE released an International Standard—CIE S 026/E:2018 (CIE, 2018)—that includes the melanopic and rhodopic action spectra alongside the CIEPO06 cone action spectra and outlines best practices for documenting photoreceptor responses to light.

With an accurately calibrated multiprimary system, one can predict $E(\lambda)$, the spectral output of the device (radiance or irradiance, in photons or watts), for any combination of primary gain settings using interpolation followed by a linear combination of primary spectra. Then, with photoreceptor action spectra appropriate to the intended observer, one can compute the activation level for each class of photoreceptors following the equation:

$$E_\alpha = \sum_{380}^{780} E(\lambda)S_\alpha(\lambda)\Delta_\lambda$$

Equation 1. Calculating α-opic irradiance

where E_α is a scalar representing the photoreceptor activation for photoreceptor class α (e.g., one of the five photoreceptors: S cones, M cones, L cones, rods, ipRGCs), $S_\alpha(\lambda)$ is the

estimated photoreceptor action spectrum, and Δ_λ is the width of the spectral sampling. By convention (CIE, 2018; Lucas et al., 2014), when this computation concerns the spectral sensitivity functions of retinal photoreceptors, the resulting measures may be called α-opic irradiance. Figure 3 shows an example spectral measurement alongside the α-opic action spectra and the resulting α-opic irradiance measures that follow from Equation 1.
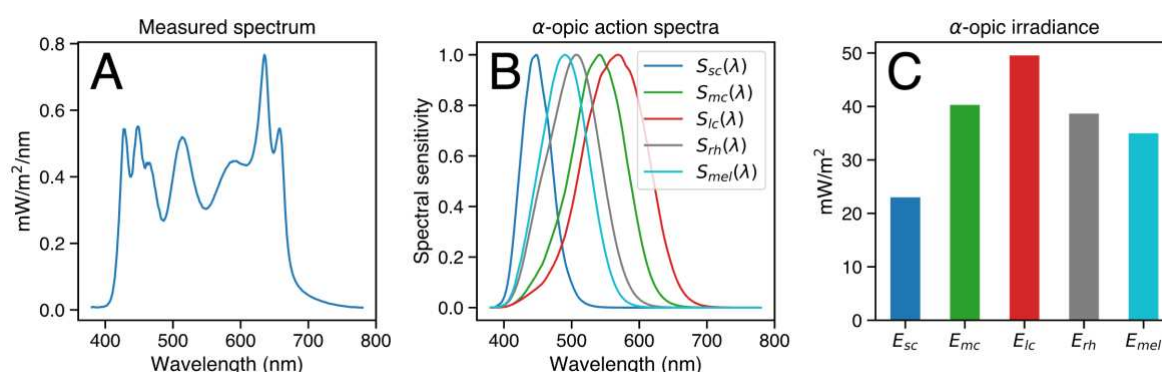

Figure 3. Calculating α-opic irradiance in accordance with CIE S 026 (CIE, 2018). (A) A spectral measurement is weighted against each of the (B) photoreceptor sensitivity functions to obtain (C) the respective α-opic quantities, following Equation 1.

The goal of silent substitution is to invert this process to determine the device input settings to produce two spectra—a background spectrum and a modulation spectrum—where the resulting α-opic quantities will be the same for all but the targeted photoreceptor(s). In the case where linearity holds across the entire α-opic computation, silent substitution is typically computed using linear algebra, by inverting a fully- or over-determined set of equations describing the mapping from primaries to photoreceptor responses (e.g., Cao et al., 2015; Maguire et al., 2016; Shapiro et al., 1996). However, where linearity fails at some point in the system (for example, if the spectrum of a particular primary changes as a function of its intensity) then it may still be possible to obtain a solution using constrained numerical optimisation (e.g., Spitschan et al., 2015).

In this Methods paper we introduce *PySilSub* (Martin et al., 2023), a Python toolbox that eases the computational burden of silent substitution by taking a structured approach to dealing with the various confounds and challenges outlined above. The toolbox provides

PYTHON TOOLBOX FOR SILENT SUBSTITUTION

flexible object-oriented support for multiprimary stimulation devices and individual colorimetric observer models, example calibration data for a range of devices, an intuitive interface for defining and solving silent substitution problems with linear algebra and constrained numerical optimization, and methods for accessing relevant standards and visualising solutions. The code is actively maintained on GitHub (https://github.com/PySilentSubstitution/pysilsub) under the MIT License and comes with a comprehensive testing suite and extensive online documentation with detailed examples. It is also registered with the Python Package Index (https://pypi.org/project/pysilsub/) and can therefore be installed with the *pip* packaging tool. Here, we provide an overview of the toolbox, describe key features, and demonstrate how it can be used.

Overview

PySilSub (Martin et al., 2023) is written in *Python3* and depends on widely used libraries from the scientific Python ecosystem (*numpy*: Harris et al., 2020; *matplotlib*: Hunter, 2007; *pandas*: McKinney, 2010; *scipy*: Virtanen et al., 2020) as well as some functionality from the *colour-science* package (Mansencal et al., 2022). Three core modules support colorimetric observer models (observers.py), multiprimary stimulation devices (devices.py), and defining, solving and visualising silent substitution problems (problems.py). Additional modules support CIE standards (CIE.py), prereceptoral filters (preceps.py), color computations (colorfuncs.py) and stimulus design (waves.py). Figure 4 lays out the anatomy of the package and highlights key features. The following sections describe the rationale and implementation of the core modules and key features.
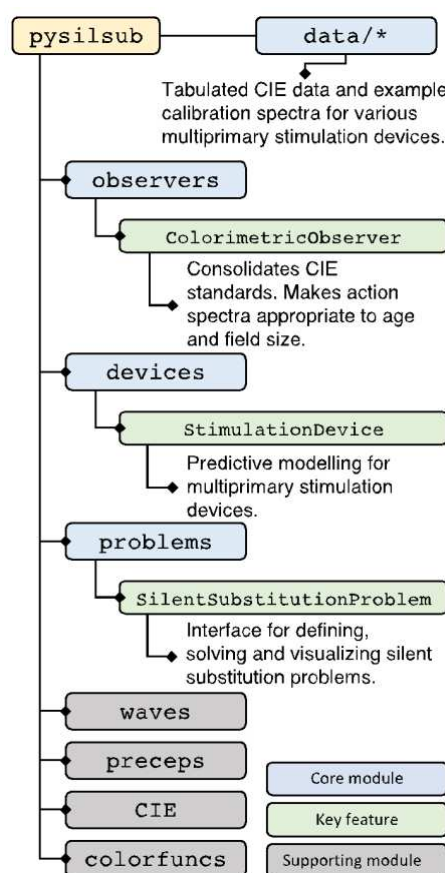
PYTHON TOOLBOX FOR SILENT SUBSTITUTION

Figure 4. Anatomy and key features of *PySilSub*.

Colorimetric observers (*observers.py*)

PySilSub consolidates the CIEOP06 (CIE, 2006) and CIE S 026 (CIE, 2018) observers in a *ColorimetricObserver* class that internally computes photoreceptor action spectra appropriate to a given age and field size. LMS cone fundamentals are constructed from the photopigment absorbance spectra (Stockman & Sharpe, 2000), taking account of the peak axial density of the respective photopigments, as well as lens (Pokorny et al., 1987; Stockman et al., 1999; Stockman & Sharpe, 2000) and macular pigment (Bone et al., 1988; Stockman et al., 1999) density, in accordance with the CIEPO06 model (CIE, 2006). The melanopic and rhodopic action spectra of the 32-year-old standard observer are taken from CIE S 026 (CIE, 2018) and adjusted for lens transmittance with a spectral correction function, in accordance with the standard. Note that for consistency with the melanopic existing standards, a slightly different lens density function is used by default to correct the

melanopic and rhodopic action spectra (for more information, see CIE S 026, CIE, 2018).

Macular pigment correction is not applied to the rhodopic and melanopic action spectra as

rods are not present at the fovea and ipRGCs are positioned above the retinal pigment layer

(Trieschmann et al., 2008).

The *ColorimetricObserver* class stores the photoreceptor action spectra in a *pandas DataFrame* (McKinney, 2010) which interacts with other parts of the toolbox as required. An advantage of this approach is that it enables the software to flexibly adapt to scenarios that may require alternative action spectra, such as targeting cones in the shadow of retinal blood vessels (Figure 5, C: Adams & Horton, 2002; Spitschan et al., 2015), performing silent substitution with non-human animals (Figure 5, D: e.g., Allen & Lucas, 2016; Mouland et al., 2019, 2021; Wise et al., 2021), or using alternative action spectra for any conceivable reason, in which case one need only create a modified observer class with the relevant photoreceptor action spectra (see examples online). Incidentally, the *ColorimetricObserver* class is also a convenient open-source means of obtaining a full set of tabulated CIEPO06- and CIE S 026-compliant photoreceptor action spectra for a human observer for any age between 20 and 80 years and for any field size from 2° to 10°.
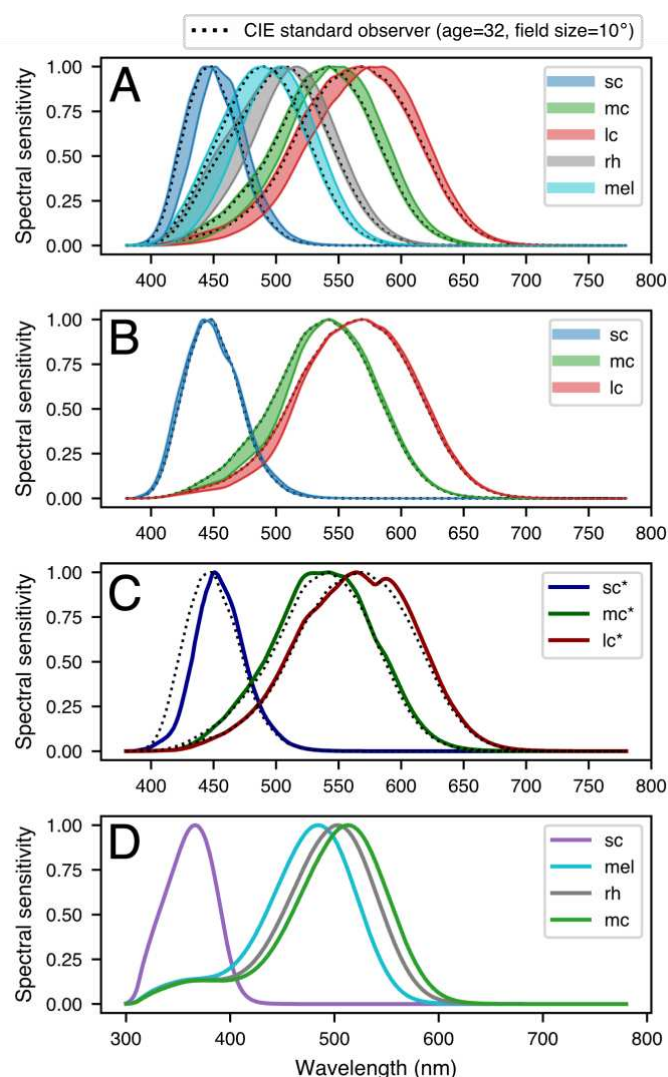
Figure 5. Spectral sensitivity of photoreceptors depends on the ocular physiology of the observer. (A) Lens yellowing with age causes a rightward shift in peak sensitivity of photopigments and alters the overall shape of sensitivity functions (shaded areas show the range of the spectral shift for ages 20 to 80 years). (B) Decreasing stimulus field size causes a small shift in S-cone sensitivity and a marked dampening of the left-hand slopes of the sensitivity functions for M- and L-cones (shaded areas show the range of the spectral shift for field sizes 10° to 2°). Note that the effects of macular pigment absorption are considered negligible for rhodopsin and melanopsin, as rods are absent from the fovea and ipRGCs sit above the retinal pigment layer (Trieschmann et al., 2008). (C) Cones in the shadow of retinal blood vessels (sc*, mc*, lc*) have altered spectral sensitivity functions due to prefiltering of light by blood. Targeting these cones produces the entopic Purkinje tree percept (Adams and Horton, 2002; Spitschan et al., 2015). (D) Spectral sensitivity functions are species dependent. The example shown is for mice (from the Rodent Toolbox v2.2: Lucas et al., 2014). Note that mice do not possess a third cone and that the spectral sensitivity of photoreceptors peaks at different locations in the visual spectrum in comparison to humans. S-cone sensitivity is shifted leftwards towards the near-UV portion of the spectrum and there is increased overlap of the M-cone, melanopic and rhodopic action spectra.

Multiprimary stimulation devices (*devices.py*)

PYTHON TOOLBOX FOR SILENT SUBSTITUTION

PySilSub supports multiprimary stimulation devices through a generic

StimulationDevice class that turns a set of spectral calibration measurements into a forward

model. The required format of the calibration data is a CSV file where the first row describes

the wavelength sampling (e.g., 380, 381, … 780) and every other row is a spectral

measurement (see Table 1). Also required in the first row of the CSV file are the column

headers *Primary* and *Setting*, whose corresponding values identify the source of the spectral

measurements. As devices may not be linear it is prudent to obtain measurements across

the entire range of primary intensities. If sampling with an OceanOptics (Ocean Insight Inc.,

Oxford, UK) or JETI (JETI Technische Instrumente, GmbH, Jena, Germany) spectrometer,

one may be able to automate these measurements with the help of interfaces in Python

packages such as *LuxPy* (Smet, 2020), *Seabreeze* (Poehlmann, 2019) and our own *PyPlr*

(Martin et al., 2021; Martin & Spitschan, 2021).

Table 1. Calibration file format. A minimal example is shown for a hypothetical 4-primary device with 8-bit resolution. Each primary is assigned an ordinal index starting at zero and has a spectral measurement for the maximum (255) and minimum (0) input setting, where the minimum setting should reflect the ambient spectral power distribution (i.e., when all channels are off). A reasonable number of intermediary measurements should also be included to account for non-linearity in the device.

Wavelength		380	381	…	779	780
Primary	Setting					
0	0					
0	…					
0	255					
1	0					
1	…			*Spectral measurements -->*		
1	255					
2	0					
2	…					
2	255					

PYTHON TOOLBOX FOR SILENT SUBSTITUTION

3	0	
3	…	
3	255	

StimulationDevice has methods for predicting and visualizing the spectral and colorimetric output of a device. Predictive methods respond to native device settings (e.g., 0-255 for a device with 8-bit resolution) or floating-point input weights between 0.0 and 1.0. The basis of all forward-predictions is a method called *.predict_primary_spd(…)* which uses input-wise linear interpolation on the calibration spectra to predict the spectral output for a given primary at a given setting. A similar method called *.predict_multiprimary_spd(…)* sums the output of repeated calls to the previous method to predict the spectral output for a full sequence of primary inputs. Following the same pattern, *.predict_multiprimary_aopic(…)* computes a mutiprimary spectrum and returns the predicted α-opic irradiances for the assigned observer. By default, this is the CIEPO06 Standard Observer (age=32, field size=10°), but a custom observer may be assigned when building the class. Additional methods make it easy to perform gamma correction, change back and forth between weights and settings, visualize the calibration SPDs and gamut of the device, and instantiate from a preconfigured JSON file. Note that *PySilSub* includes example data for a range of multiprimary systems (Figure 6), which makes it easy to explore how the toolbox functions without having to develop one's own system.
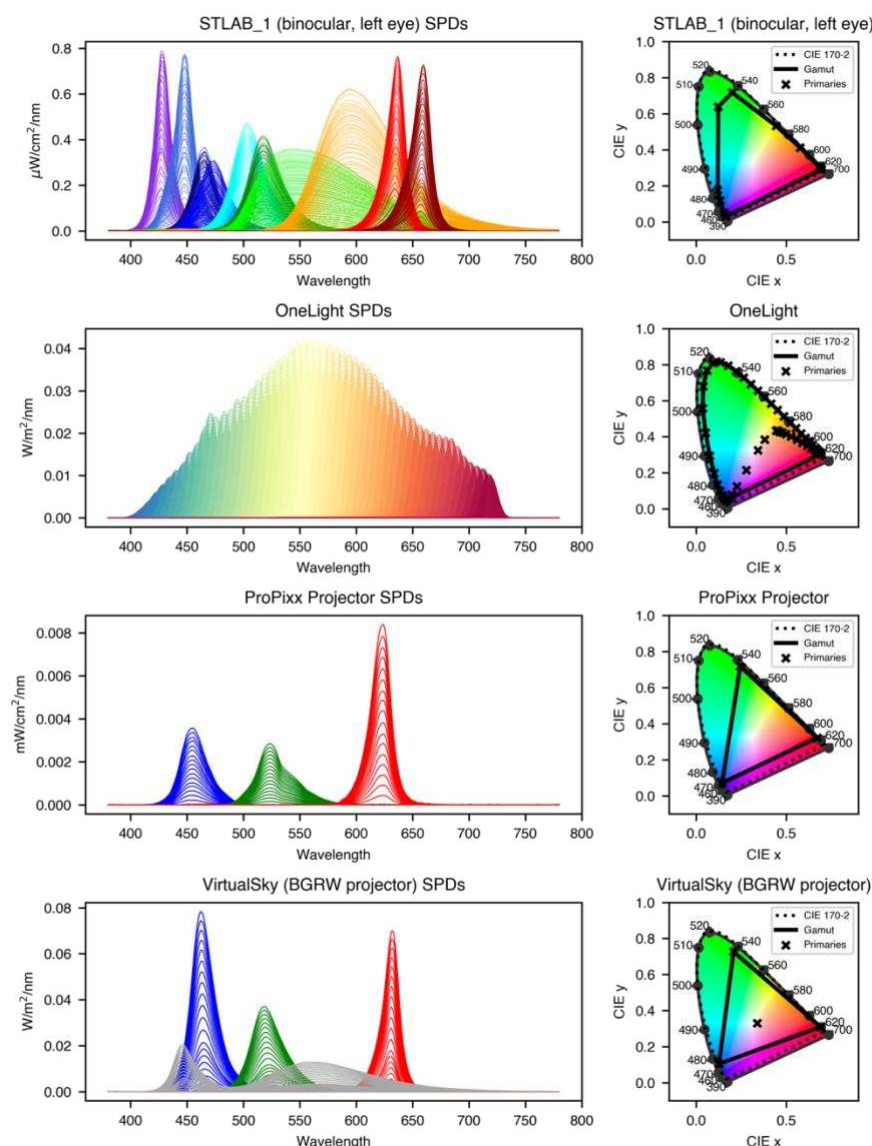
PYTHON TOOLBOX FOR SILENT SUBSTITUTION

Figure 6. Example package data for multiprimary systems: (A) SpectraTuneLab 10-primary light engine (LEDMOTIVE technologies, LLC, Barcelona, Spain), (B) VISX Spectra Digital Light Engine (OneLight Corporation, Vancouver, Canada; calibration spectra from Spitschan et al., 2015), (C) VPixx ProPixx projector (VPixx Technologies Inc., Quebec, Canada), (D) BGRW VirtualSky (Fraunhofer IAO, Stuttgart, Germany; Stefani et al., 2012).

Silent substitution problems (*problems.py*)

Stimuli in a silent substitution protocol typically take the form of pulses (e.g., Maguire et al., 2017; McAdams et al., 2018) or sinusoidal modulations (e.g., Barrionuevo et al., 2018; Spitschan et al., 2014) of photoreceptor-directed contrast presented against a background spectrum to which an observer has adapted. The background spectrum serves to maintain a set pattern of photoreceptor activations and the modulation spectrum increases activation of

the targeted photoreceptor(s) without altering activation of the others. Finding the native device inputs for these theoretical background and modulation spectra is a computational problem whose definition depends on one's research aims and stimulus requirements. Above all, one must nominate which photoreceptor(s) to target, which to silence, and which to ignore (if any, see discussion), but it may also be advantageous to refine the problem by specifying a particular background spectrum, how much contrast to aim for on the targeted photoreceptor(s), and whether to impose any bounds on the primary inputs. These decisions then guide the development of a computational algorithm whose execution will return a solution—a set of native device settings for the background and modulation spectra—that satisfies the constraints in the problem specification.

With *PySilSub*, this process is streamlined by a *SilentSubstitutionProblem* class that inherits from *StimulationDevice*, has a *ColorimetricObserver* assigned to it, and incorporates properties for defining, and methods for solving and visualizing, silent substitution problems. After instantiating, a problem is conditioned by setting several basic and well-documented properties (i.e., managed attributes), including which photoreceptors to target, silence and ignore, and optionally the background spectrum, target contrast and primary input bounds. A solution is then obtained with a call to one of the two solver methods described below (see Figure 7 for a set of examples).

Linear algebra: .linalg_solve().

Linear algebra is a fast and efficient means of solving silent substitution problems (Cao et al., 2015; Evéquoz et al., 2021; Shapiro et al., 1996). The *.linalg_solve()* method applies specifically for situations where the background spectrum and target contrast are already known. To illustrate how it works, suppose we have a 5-primary system and that for a background spectrum we wish to use the mixture of all primaries at half-power, $\alpha_{bg} =$ [.5 .5 .5 .5 .5]. First, we generate the matrix P_{bg}, where the rows of P_{bg} are the predicted spectral power distribution for each primary component of the background spectrum $P_{bg} =$ [$p_1(\lambda)\ p_2(\lambda)\ p_3(\lambda)\ p_4(\lambda)\ p_5(\lambda)$]. We then compute the matrix of α-opic irradiances:

$$A = P_{bg} \cdot S_\alpha$$

where the columns of S_α are the photoreceptor action spectra of the observer, $S_\alpha = [sc(\lambda)\ mc(\lambda)\ lc(\lambda)\ rh(\lambda)\ mel(\lambda)]^T$. Given a set of scaling coefficients for the primaries, $\alpha_{sc} = [p_1\ p_2\ p_3\ p_4\ p_5]$, the forward model predicts that the output modulation $\beta = [sc\ mc\ lc\ rh\ mel]$ is $\beta = \alpha_{sc}A$. To invert this process, we calculate $\alpha_{sc} = \beta A^{-1}$, which provides the desired scaling coefficients that must be added to the primary weights for the background in order to produce the desired output modulation β. Finally, the solution is given as, $\alpha_{mod} = \alpha_{bg} + \alpha_{sc}$.

The *.linalg_solve()* method relies on functionality from *numpy*'s *linalg* module (Harris et al., 2020). Specifically, in the case of square matrices (e.g., five primaries and five photoreceptors) the *inv* function is used to perform matrix inversion, whereas non-square (i.e., overdetermined) matrices require the *pinv* (Moore-Penrose pseudo-inverse) function, which finds the least squares solution.

Constrained numerical optimization: .optim_solve().

Linear algebra cannot provide a direct solution in the case where nonlinearities exist in the forward model. An example of this occurs when the spectrum of the primaries changes as a function of their intensity. In this case, it is still possible to obtain a solution through a numerical search procedure by solving a multi-dimensional error minimization problem of the form:

$$\begin{aligned} \underset{x \in \mathbb{R}^n}{\text{minimize}} \quad & f(x) \\ \text{subject to} \quad & g^L \le g(x) \le g^U \\ & x^L \le x \le x^U, \end{aligned}$$

Equation 2. Constrained numerical optimization.

where $x \in R^n$ are the optimization variables (i.e., the primary input weights) whose lower and upper bounds, x^L and x^U, are between 0 and 1 to ensure that the solution is within the gamut of the device; $f(x)$ is the objective function (which in this case is a class method that is conditioned through setting the properties outlined above) that aims to maximize contrast

on the target photoreceptor(s); and $g(x)$ is a constraint function (also a class method) that calculates contrast for the nominally silenced photoreceptor(s), where g^L and g^U should be zero. In all cases, x is a vector containing the primary input weights for the proposed modulation spectrum (and the background spectrum if it is not specified).

By default, *.optim_solve()* performs a local optimization from a random starting point on the function landscape using *scipy*'s (Virtanen et al., 2020) *minimize* function with the *SLSQP* (Sequential Least Squares Quadratic Programming) solver. The method may also be instructed via a keyword argument to perform a global search with *scipy*'s *basinhopping* algorithm, in which case a series of local optimisations are performed in conjunction with a global stepping algorithm and the best solution returned (Olson et al., 2012). Optimization parameters are preconfigured with sensible values, but may be changed via keyword arguments, and for full flexibility one can set up an optimization externally and pass it the objective and constraint functions from the problem class. As well as permitting the solution to silent substitution problems in cases where there are nonlinearities in the forward model, the *.optim_solve()* method is also a convenient way to identify background and modulation spectra that maximize unipolar amplitudes along a particular direction in photoreceptor space.
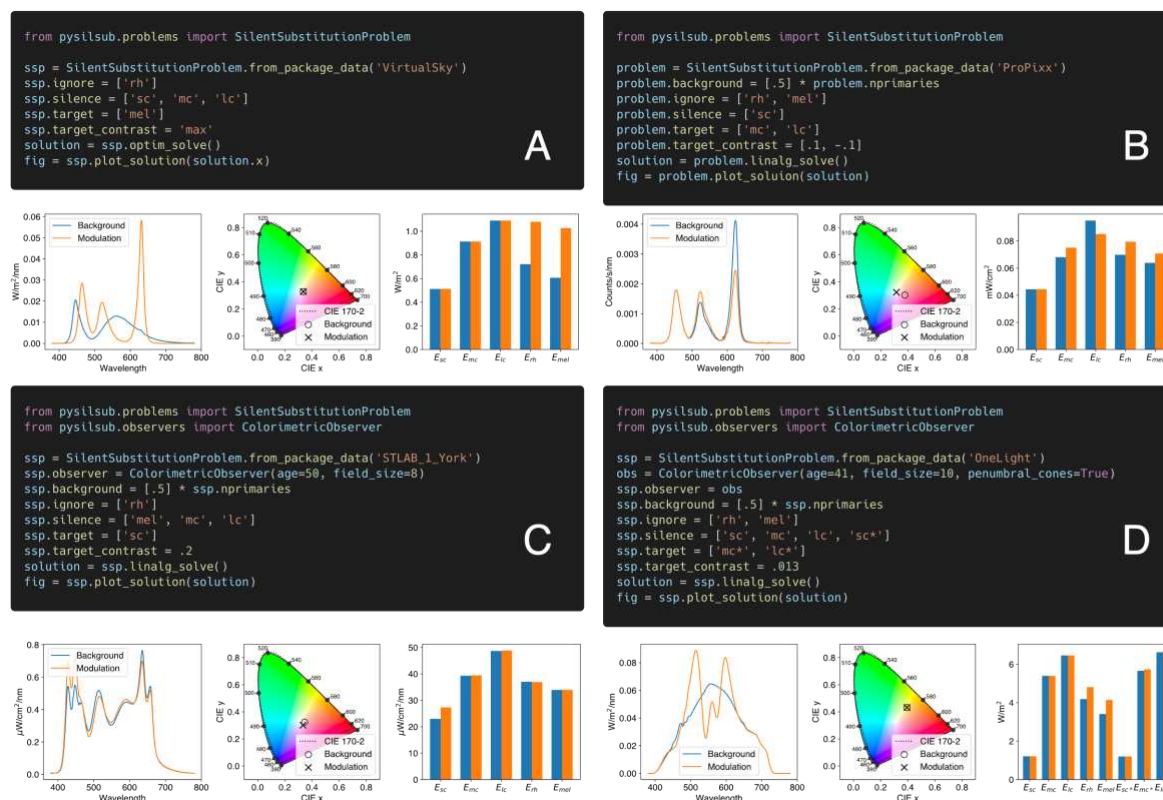
Figure 7. Defining and solving silent substitution problems with *PySilSub*'s example package data. (A) Using a BGRW VirtualSky (Fraunhofer IAO, Stuttgart, Germany; Stefani et al., 2012) to maximize melanopic contrast whilst ignoring rods and minimizing cones. Solved with numerical optimization without having specified a background spectrum (the background is optimized and included in the solution). (B) Using a VPixx ProPixx projector to target the L-M postreceptoral pathway whilst minimizing S cone contrast and ignoring rods and melanopsin, against a background spectrum defined as each of the three primaries at their half-maximum setting. Solved with linear algebra. (C) Using a SpectraTuneLAB 10-primary light engine (LEDMOTIVE technologies, LLC, Barcelona, Spain) to target S cones with 20% contrast, for a 50-year-old observer and field size of 8 degrees, whilst ignoring rods and minimizing melanopsin and M- /L-cones, against a background spectrum defined as all primaries at their half-maximum setting. Solved with linear algebra. (D) Using a VISX Spectra Digital Light Engine (OneLight Corporation, Vancouver, Canada; calibration spectra from Spitschan et al., 2015) to target M- and L-cones in the shadow of retinal blood vessels for a 41-year-old observer and a field size of 10 degrees.

Discussion

First described by Estévez and Spekreijse (1982), the method of silent substitution involves using a spectral stimulation system with multiple independent primaries to selectively stimulate one class (or multiple classes) of retinal photoreceptor whilst maintaining a constant level of activation in the others. To apply the method, one must acquire a multiprimary stimulation system (for guidance, see Conus & Geiser, 2020) and accurate calibration spectra for the independent primaries. Photoreceptor action spectra appropriate to the intended observer are also required so that the spectral output of the system may be quantified in terms of α-opic irradiance—the amount of light 'seen' by the individual photoreceptor classes. After nominating which photoreceptor(s) to target and which to silence (in accordance with research aims), the goal of silent substitution is to find the device input settings for a background spectrum and a modulation spectrum who's predicted α-opic irradiances are the same for the silenced but not for the targeted photoreceptor(s). In practice, this is a computational problem that must take account of various confounds and challenges, chief among which are inter- and intra-observer variabilities in ocular physiology (i.e., lens and macular pigment density) and the reliability and linearity of the stimulation device (Spitschan & Woelders, 2018). To support our ongoing research with a dual multiprimary binocular system, we produced software that streamlines much of the above process and eases the computational burden of silent substitution, generally making it easy to define, solve and visualize observer- and device-specific problems. Our efforts resulted in *PySilSub*, an open-source, *pip*-installable Python toolbox for implementing the method of silent substitution in vision and nonvisual photoreception research.

The first key feature of our software is *pysilsub.observers.ColorimetricObserver*, which computes and stores photoreceptor action spectra appropriate to observer age (20 to 80 years) and stimulus field size (1° to 10°) in accordance with the CIEPO06 (CIE, 2006) and CIE S 026 (CIE, 2018) observer models. Previous studies vary considerably in the

photoreceptor action spectra that are assumed for observers (Spitschan & Woelders, 2018, Table 1), which may in part be due to the difficulty in obtaining full sets of CIE-compliant action spectra. Although versions of these data are maintained at various locations on the web (e.g., www.cvrl.com) or can be accessed or computed from openly available software implementations (Asano et al., 2016; Price et al., 2020; Smet, 2020), we found no single implementation that provides a full set of photoreceptor action spectra—cones, rods and ipRGCs—appropriate to a given age and field size. This inspired us to develop our own implementation which in turn enables us to natively support silent substitution for the vast majority of human colorimetric observers. To our knowledge, this is one of few open-source methods of obtaining photoreceptor action spectra appropriate to observer age and stimulus field size, and for this reason has broad relevance in color and vision science, not just silent substitution.

The next key feature of our software is *pysilsub.devices.StimulationDevice*, which serves as a forward model for any multiprimary stimulation system for which accurate spectral calibration data are available. Various methods allow for output to be predicted for both independent primaries and multiple primaries. By default, α-opic irradiances are computed for the CIE Standard Physiological Observer, but if a custom observer is assigned, the appropriate action spectra will be used for the calculations. This aspect of the software is best thought of as a predictive engine that performs the basic computations underlying silent substitution. As such, the output is only as a good as the input, and it is important to ensure that the calibration spectra are representative of what an observer actually sees, that they are obtained with a wavelength- and irradiance-calibrated spectrometer, and that the wavelength sampling resolution agrees with that of the observer action spectra.

pysilsub.problems.SilentSubstitutionProblem acts as an interface for defining, solving and visualizing silent substitution problems for a given observer and stimulation device. A problem is first conditioned by specifying which photoreceptors to ignore, silence and target, and optionally a background spectrum, the target contrast, and any restrictive bounds on the

primary inputs. A solution to the problem is then obtained via a call to one of two solver methods based either on linear algebra or on constrained numerical optimization. It is important to note that the behavior of the solvers depends on the values that were set for the aforementioned properties. This is an intuitive, albeit non-standard, design pattern that facilitates quick and easy experimentation as compared to calling functions with long lists of arguments. The predicted spectral power distribution, chromaticity coordinates, and α-opic irradiances for the background and modulation spectra of a solution can be visualized via a single method call (e.g., see Figure 7) and likewise converted to native device settings when ready for use in an experiment.

The ability to ignore photoreceptors has practical advantages. For example, if studying cone-mediated vision with a standard RGB display, one could ignore both rods and melanopsin to precompute cone contrast settings for use with stimulus display software such as the Psychophysics Toolbox (Brainard, 1997; Kleiner et al, 2007) or PsychoPy (Peirce et al, 2009). If performing silent substitution in dichromats (e.g., Huchzermeyer et al., 2018; Kremers et al., 1999; Usui et al., 1998) one can simply ignore the non-functioning cone class. Similarly, if administering stimuli in the photopic range, one may wish to ignore rod photoreceptors, which are often assumed to be incapable of signaling above certain light levels (see Adelson, 1982; Aguilar & Stiles, 1954). In latter cases, ignoring the inactive photoreceptor(s) will allow for more contrast to be directed towards the targeted photoreceptor(s). Imposing limits on the primary bounds is another convenient feature that can be used to ensure that solutions avoid the hard edges of a device's gamut, which may recede as the device ages (this is especially the case with LED-based systems).

As a final note, we stress that *PySilSub* is a generic software for dealing with the computational aspect of a challenging vision science technique. Researchers should take the usual care when designing, planning, and interpreting the results of an experiment. Accurate calibration spectra are an essential requirement to valid solutions, and it is always prudent to obtain validation measurements for a solution to ensure that the actual α-opic irradiances are as predicted by the software. When interpreting the results of an experiment,

researchers should acknowledge that silencing photoreceptors at the pigment level does not necessarily silence photoreceptor output (Kamar et al., 2019). The complex circuitry of the retina is such that cone cells receive feedback from other cells via horizontal cells, which means that receptor output is not dependent on quantum catch alone. That said, there is converging evidence from human experiments that the method of silent substitution can yield highly specific, photoreceptor-level characterizations. In their recent protocol paper, Nugent et al. (2023) provide a comprehensive treatment of the method of silent substitution covering also display development, calibration, and potential methods to fine-tune stimuli to individual-observer characteristics.

To conclude, we have developed an open-source Python toolbox for implementing the method of silent substitution in vision and nonvisual photoreception research. For further information on the software, we refer readers to its GitHub repository (https://github.com/PySilentSubstitution/pysilsub) and online documentation pages (https://pypi.org/project/pysilsub/). Feedback and contributions in the form of issues and pull requests are warmly encouraged.

Acknowledgements

References

Adams, D. L., & Horton, J. C. (2002). Shadows cast by retinal blood vessels mapped in primary visual cortex. *Science*, *298*(5593), 572-576. https://doi.org/10.1126/science.107488

Adelson, E. H. (1982). Saturation and Adaptation. *Vision Research*, *22*, 1299–1312.

Aguilar, M., & Stiles, W. S. (1954). Saturation of the rod mechanism of the retina at high levels of stimulation. *Optica Acta: International Journal of Optics*, *1*(1), 59–65. https://doi.org/10.1080/713818657

Al Enezi, J., Revell, V., Brown, T., Wynne, J., Schlangen, L., & Lucas, R. J. (2011). A "melanopic" spectral efficiency function predicts the sensitivity of melanopsin photoreceptors to polychromatic lights. *Journal of Biological Rhythms*, *26*(4), 314–323. https://doi.org/10.1177/0748730411409719

Allen, A. E., Hazelhoff, E. M., Martial, F. P., Cajochen, C., & Lucas, R. J. (2018). Exploiting metamerism to regulate the impact of a visual display on alertness and melatonin suppression independent of visual appearance. *Sleep*, *41*(8), 1–7. https://doi.org/10.1093/sleep/zsy100

Allen, A. E., Martial, F. P., & Lucas, R. J. (2019). Form vision from melanopsin in humans. *Nature communications*, *10*(1), 2274. https://doi.org/10.1038/s41467-019-10113-3

Allen, A. E., & Lucas, R. J. (2016). Using silent substitution to track the mesopic transition from rod- to cone-based vision in mice. *Investigative Ophthalmology and Visual Science*, *57*(1), 276–287. https://doi.org/10.1167/iovs.15-18197

Asano, Y., Fairchild, M. D., & Blondé, L. (2016). Individual colorimetric observer model. *PLoS ONE*, *11*(2), 1–19. https://doi.org/10.1371/journal.pone.0145671

Barrionuevo, P. A., McAnany, J. J., Zele, A. J., & Cao, D. (2018). Non-linearities in the rod and cone photoreceptor inputs to the afferent pupil light response. *Frontiers in Neurology*, *9*(December), 1–8. https://doi.org/10.3389/fneur.2018.01140

Barrionuevo, P. A., Preciado, O. U., ML, S. S., & Issolio, L. A. (2022). Optical stimulation systems for studying human vision. *Progress in brain research*, *273*(1), 13-36.

https://doi.org/10.1016/bs.pbr.2022.04.003

Baylor, D. A., Nunn, B. J., & Schnapf, J. L. (1984). The photocurrent, noise and spectral sensitivity of rods of the monkey Macaca fascicularis. *The Journal of Physiology*, *357*(1), 575–607. https://doi.org/10.1113/jphysiol.1984.sp015518

Berson, D. M., Dunn, F. A., & Takao, M. (2002). Phototransduction by retinal ganglion cells that set the circadian clock. *Science*, *295*(5557), 1070–1073. https://doi.org/10.1126/science.1067262

Blume, C., Garbazza, C., & Spitschan, M. (2019). Effects of light on human circadian rhythms, sleep and mood. *Somnologie*, *23*(3), 147–156. https://doi.org/10.1007/s11818-019-00215-x

Blume, C., Niedernhuber, M., Spitschan, M., Slawik, H. C., Meyer, M. P., Bekinschtein, T. A., & Cajochen, C. (2022). Melatonin suppression does not automatically alter sleepiness, vigilance, sensory processing, or sleep. *Sleep*, *45*(11), November 2022, zsac199. https://doi.org/10.1093/sleep/zsac199

Bone, R. A., Landrum, J. T., Fernandez, L., & Tarsis, S. L. (1988). Analysis of the macular pigment by HPLC: Retinal distribution and age study. *Investigative Ophthalmology and Visual Science*, *29*(6), 843–849. https://iovs.arvojournals.org/article.aspx?articleid=2160043

Bowmaker, J. K., & Dartnall, H. J. (1980). Visual pigments of rods and cones in a human retina. *The Journal of Physiology*, *298*(1), 501–511. https://doi.org/10.1113/jphysiol.1980.sp013097

Bowmaker, J. K., Dartnall, H. J., Lythgoe, J. N., & Mollon, J. D. (1978). The visual pigments of rods and cones in the rhesus monkey, Macaca mulatta. *The Journal of Physiology*, *274*(1), 329–348. https://doi.org/10.1113/jphysiol.1978.sp012151

Brainard, D. H., & Vision, S. (1997). The psychophysics toolbox. *Spatial vision*, *10*(4), 433-436. https://doi.org/10.1163/156856897X00357

Brown, T. M., Allen, A. E., Al-Enezi, J., Wynne, J., Schlangen, L., Hommes, V., & Lucas, R. J. (2013). The melanopic sensitivity function accounts for melanopsin-driven responses

in mice under diverse lighting conditions. *PLoS ONE*, *8*(1), 1–8.

https://doi.org/10.1371/journal.pone.0053583

Brown, T. M., Tsujimura, S., Allen, A. E., Wynne, J., Bedford, R., Vickery, G., Vugler, A., & Lucas, R. J. (2012). Melanopsin-based brightness discrimination in mice and humans. *Current biology : CB*, *22*(12), 1134–1141. https://doi.org/10.1016/j.cub.2012.04.039

Cao, D., Nicandro, N., & Barrionuevo, P. A. (2015). A five-primary photostimulator suitable for studying intrinsically photosensitive retinal ganglion cell functions in humans. *Journal of Vision*, *15*(1), 1–13. https://doi.org/10.1167/15.1.27

Chen, S. F., Chang, Y., & Wu, J. C. (2001). The spatial distribution of macular pigment in humans. *Current Eye Research*, *23*(6), 422–434. https://doi.org/10.1076/ceyr.23.6.422.6963

CIE. (2006). Fundamental chromaticity diagram with physiological axes. In *CIE Technical Report*. https://cie.co.at/publications/fundamental-chromaticity-diagram-physiological-axes-part-1

CIE. (2018). *CIE System for Metrology of Optical Radiation for ipRGC-Influenced Responses to Light.* CIE Central Bureau.

Conus, V., & Geiser, M. (2020). A review of silent substitution devices for melanopsin stimulation in humans. *Photonics*, *7*(4), 1–10. https://doi.org/10.3390/photonics7040121

Dacey, D. M., Liao, H. W., Peterson, B. B., Robinson, F. R., Smith, V. C., Pokorny, J., Yau, K. W., & Gamlin, P. D. R. (2005). Melanopsin-expressing ganglion cells in primate retina signal colour and irradiance and project to the LGN. *Nature*, *433*(7027), 749–754. https://doi.org/10.1038/nature03344

DeLawyer, T., Tsujimura, S. I., & Shinomori, K. (2020). Relative contributions of melanopsin to brightness discrimination when hue and luminance also vary. *JOSA A*, *37*(4), A81-A88. https://doi.org/10.1364/JOSAA.382349

Estévez, O., & Spekreijse, H. (1982). The " Silent Substitution " method in research. *Vision Research*, *22*(6), 681–691. https://doi.org/10.1016/0042-6989(82)90104-3

Evéquoz, G., Truffer, F., & Geiser, M. (2021). Maximum possible contrast level for silent

substitution: a theoretical model applied to melanopsin stimulation. *Journal of the Optical Society of America A*, *38*(9), 1312. https://doi.org/10.1364/josaa.420373

Feldman, B. H., Heersink, S., Patel, A. S., DelMonte, D. W., Hossain, K., Baartman, B., Anderson, D., & Stelzner, S. K. (2022). *Cataract*. American Academy of Ophthalmology. https://eyewiki.aao.org/Cataract

Gamlin, P. D. R., McDougal, D. H., Pokorny, J., Smith, V. C., Yau, K. W., & Dacey, D. M. (2007). Human and macaque pupil responses driven by melanopsin-containing retinal ganglion cells. *Vision Research*, *47*(7), 946–954. https://doi.org/10.1016/j.visres.2006.12.015

Grünert, U., & Martin, P. R. (2020). Cell types and cell circuits in human and non-human primate retina. *Progress in Retinal and Eye Research*, *78*(November 2019), 100844. https://doi.org/10.1016/j.preteyeres.2020.100844

Harris, C. R., Millman, K. J., van der Walt, S. J., Gommers, R., Virtanen, P., Cournapeau, D., Wieser, E., Taylor, J., Berg, S., Smith, N. J., Kern, R., Picus, M., Hoyer, S., van Kerkwijk, M. H., Brett, M., Haldane, A., del Río, J. F., Wiebe, M., Peterson, P., … Oliphant, T. E. (2020). Array programming with NumPy. *Nature*, *585*(7825), 357–362. https://doi.org/10.1038/s41586-020-2649-2

Hexley, A. C., Yöntem, A. Ö., Spitschan, M., Smithson, H. E., & Mantiuk, R. (2020). Demonstrating a multi-primary high dynamic range display system for vision experiments. *JOSA A*, *37*(4), A271-A284. https://doi.org/10.1364/JOSAA.384022

Horiguchi, H., Winawer, J., Dougherty, R. F., & Wandell, B. A. (2013). Human trichromacy revisited. *Proceedings of the National Academy of Sciences of the United States of America*, *110*(3). https://doi.org/10.1073/pnas.1214240110

Huchzermeyer, C., Martins, C. M. G., Nagy, B., Barboni, M. T. S., Ventura, D. F., Costa, M. F., & Kremers, J. (2018). Photoreceptor-specific light adaptation of critical flicker frequency in trichromat and dichromat observers. *Journal of the Optical Society of America A*, *35*(4), B106. https://doi.org/10.1364/josaa.35.00b106

Hunter, J. D. (2007). Matplotlib: A 2D graphics environment. *Computing in Science and*

PYTHON TOOLBOX FOR SILENT SUBSTITUTION

Engineering, *9*(3), 90–95. https://doi.org/10.1109/MCSE.2007.55

Kamar, S., Howlett, M. H. C., & Kamermans, M. (2019). Silent-substitution stimuli silence the light responses of cones but not their output. *Journal of Vision*, *19*(5), 1–11. https://doi.org/10.1167/19.5.14

Kleiner, M., Brainard, D., & Pelli, D. (2007). What's new in Psychtoolbox-3?.

Kremers, J., Czop, D., & Link, B. (2009). Rod and S-cone driven ERG signals at high retinal illuminances. *Documenta Ophthalmologica*, *118*(3), 205–216. https://doi.org/10.1007/s10633-008-9159-0

Kremers, J., Usui, T., Scholl, H. P. N., & Sharpe, L. T. (1999). Cone signal contributions to electrograms in dichromats and trichromats. *Investigative Ophthalmology and Visual Science*, *40*(5), 920–930.

Kuze, M., Morita, T., Fukuda, Y., Kondo, M., Tsubota, K., & Ayaki, M. (2017). Electrophysiological responses from intrinsically photosensitive retinal ganglion cells are diminished in glaucoma patients. *Journal of Optometry*, *10*(4), 226–232. https://doi.org/10.1016/j.optom.2016.07.004

Lerman, S. (1980). *Radiant Energy and the Eye (Vol. 1)*. Macmillan.

Lucas, R. J., Peirson, S. N., Berson, D. M., Brown, T. M., Cooper, H. M., Czeisler, C. A., Figueiro, M. G., Gamlin, P. D., Lockley, S. W., O'Hagan, J. B., Price, L. L. A., Provencio, I., Skene, D. J., & Brainard, G. C. (2014). Measuring and using light in the melanopsin age. *Trends in Neurosciences*, *37*(1), 1–9. https://doi.org/10.1016/j.tins.2013.10.004

Maguire, J., Parry, N. R. A., Kremers, J., Kommanapalli, D., Murray, I. J., & McKeefry, D. J. (2016). Rod electroretinograms elicited by silent substitution stimuli from the light-adapted human eye. *Translational Vision Science and Technology*, *5*(4). https://doi.org/10.1167/tvst.5.4.13

Maguire, J., Parry, N. R. A., Kremers, J., Murray, I. J., & McKeefry, D. (2017). The morphology of human rod ERGs obtained by silent substitution stimulation. *Documenta Ophthalmologica*, *134*(1), 11–24. https://doi.org/10.1007/s10633-017-9571-4

Mansencal, T., Mauderer, M., Parsons, M., Shaw, N., Wheatley, K., Cooper, S., Vandenberg, J. D., Canavan, L., Crowson, K., Lev, O., Leinweber, K., Sharma, S., Sobotka, T. J., Moritz, D., Pppp, M., Rane, C., Eswaramoorthy, P., Mertic, J., Pearlstine, B., … Downs, T. (2022). *Colour 0.4.2 [computer software]*. Zenodo. https://doi.org/10.5281/zenodo.7367239

Martin, J. T., Pinto, J., Bulte, D., & Spitschan, M. (2021). PyPlr: A versatile, integrated system of hardware and software for researching the human pupillary light reflex. *Behavior Research Methods*, *0123456789*. https://doi.org/10.3758/s13428-021-01759-3

Martin, J. T., & Spitschan, M. (2021). *PyPlr (v1.0.0) [computer software]*. https://doi.org/https://doi.org/10.5281/zenodo.1234

Martin, J. T., Boynton, G. M., Baker, D. H., & Wade, A., Spitschan, M. (2023). PySilSub (Version 1.0.0) [Computer software]. https://doi.org/10.5281/zenodo.1234

McAdams, H., Igdalova, A., Spitschan, M., Brainard, D. H., & Aguirre, G. K. (2018). Pulses of melanopsin-directed contrast produce highly reproducible pupil responses that are insensitive to a change in background radiance. *Investigative Ophthalmology and Visual Science*, *59*(13), 5615–5626. https://doi.org/10.1167/iovs.18-25219

McKinney, W. (2010). Data Structures for Statistical Computing in Python. *Proceedings of the 9th Python in Science Conference*, *1*(Scipy), 56–61. https://doi.org/10.25080/majora-92bf1922-00a

Mouland, J. W., Martial, F. P., Lucas, R. J., & Brown, T. M. (2021). Modulations in irradiance directed at melanopsin, but not cone photoreceptors, reliably alter electrophysiological activity in the suprachiasmatic nucleus and circadian behaviour in mice. *Journal of Pineal Research*, *70*(4), 1–12. https://doi.org/10.1111/jpi.12735

Mouland, J. W., Martial, F., Watson, A., Lucas, R. J., & Brown, T. M. (2019). Cones Support Alignment to an Inconsistent World by Suppressing Mouse Circadian Responses to the Blue Colors Associated with Twilight. *Current Biology*, *29*(24), 4260-4267.e4. https://doi.org/10.1016/j.cub.2019.10.028

Norren, D. V., & Vos, J. J. (1974). Spectral transmission of the human ocular media. *Vision

Research, *14*(11), 1237–1244. https://doi.org/10.1016/0042-6989(74)90222-3

Nugent, T. W., & Zele, A. J. (2022). A five-primary Maxwellian-view display for independent control of melanopsin , rhodopsin , and three-cone opsins on a fine spatial scale. *Journal of Vision*, *22*, 1–22.

Nugent, T. W., Carter, D. D., Uprety, S., Adhikari, P., Feigl, B., & Zele, A. J. (2023). Protocol for isolation of melanopsin and rhodopsin in the human eye using silent substitution. *STAR protocols*, *4*(1), 102126. https://doi.org/10.1016/j.xpro.2023.102126

Olson, B., Hashmi, I., Molloy, K., & Shehu, A. (2012). Basin Hopping as a General and Versatile Optimization Framework for the Characterization of Biological Macromolecules. *Advances in Artificial Intelligence*, *2012*, 1–19. https://doi.org/10.1155/2012/674832

Peirce, J. W. (2009). Generating stimuli for neuroscience using PsychoPy. *Frontiers in neuroinformatics*, 10. https://doi.org/10.3389/neuro.11.010.2008

Poehlmann, A. (2019). *Seabreeze (v1.3.0) [computer software]*. https://github.com/ap--/python-seabreeze/releases/tag/v1.3.0

Pokorny, J., Smith, V. C., & Lutze, M. (1987). Aging of the human lens. *Applied Optics*, *26*(8), 1437. https://doi.org/10.1364/ao.26.001437

Price, L. L. A., Peirson, S. N., Schlangen, L. J. M., Spitschan, M., Lang, D., & Blattner, P. (2020). *User Guide to the alpha-opic Toolbox for implementing CIE S 026.* (v1.049a). CIE Central Bureau. https://doi.org/10.25039/S026.2018.TB

Provencio, I., Rodriguez, I. R., Jiang, G., Hayes, W. P., Moreira, E. F., & Rollag, M. D. (2000). A novel human opsin in the inner retina. *Journal of Neuroscience*, *20*(2), 600–605. https://doi.org/10.1523/jneurosci.20-02-00600.2000

Rushton, W. A. H. (1972). Pigments and signals in colour vision. *The Journal of Physiology*, *220*(3), 1–31. https://doi.org/10.1113/jphysiol.1972.sp009719

Schöllhorn, I., Stefani, O., Lucas, R. J., Spitschan, M., Slawik, H. C., & Cajochen, C. (2023). Melanopic irradiance defines the impact of evening display light on sleep latency, melatonin and alertness. *Communications Biology*, *6*(1), 228.

https://doi.org/10.1038/s42003-023-04598-4

Shapiro, A. G. (2002). Cone-specific mediation of rod sensitivity in trichromatic observers. *Investigative Ophthalmology and Visual Science*, *43*(3), 898–905.

Shapiro, A. G., Pokorny, J., & Smith, V. C. (1996). Cone – rod receptor spaces with illustrations and light-emitting-diode spectra EVALUATION OF ROD EXCITATION. *Journal of the Optical Society of America*, *13*(12), 2319–2328.

Sharpe, L. T., Fach, C., Nordby, K., & Stockman, A. (1989). The incremental threshold of the rod visual system and Weber's law. *Science*, *244*(4902), 354–356. https://doi.org/10.1126/science.2711186

Smet, K. A. G. (2020). Tutorial: The LuxPy Python Toolbox for Lighting and Color Science. *LEUKOS - Journal of Illuminating Engineering Society of North America*, *16*(3), 179–201. https://doi.org/10.1080/15502724.2018.1518717

Smith, V. C., & Pokorny, J. (1975). Spectral sensitivity of the foveal cone photopigments between 400 and 500 nm. *Vision Research*, *15*(2), 161–171. https://doi.org/10.1016/0042-6989(75)90203-5

Souman, J. L., Borra, T., de Goijer, I., Schlangen, L. J., Vlaskamp, B. N., & Lucassen, M. P. (2018). Spectral tuning of white light allows for strong reduction in melatonin suppression without changing illumination level or color temperature. *Journal of biological rhythms*, *33*(4), 420-431. https://doi.org/10.1177/0748730418784041

Spitschan, M. (2019). Melanopsin contributions to non-visual and visual function. *Current opinion in behavioral sciences*, *30*, 67-72. https://doi.org/10.1016/j.cobeha.2019.06.004

Spitschan, M., Aguirre, G. K., & Brainard, D. H. (2015). Selective stimulation of penumbral cones reveals perception in the shadow of retinal blood vessels. *PLoS ONE*, *10*(4), 1–22. https://doi.org/10.1371/journal.pone.0124328

Spitschan, M., Bock, A. S., Ryan, J., Frazzetta, G., Brainard, D. H., & Aguirre, G. K. (2017). The human visual cortex response to melanopsin-directed stimulation is accompanied by a distinct perceptual experience. *Proceedings of the National Academy of Sciences*, *114*(46), 12291-12296. https://doi.org/10.1073/pnas.1711522114

Spitschan, M., Gardasevic, M., Martial, F. P., Lucas, R. J., & Allen, A. E. (2019). Pupil responses to hidden photoreceptor-specific modulations in movies. *PloS one*, *14*(5), e0216307. https://doi.org/10.1371/journal.pone.0216307

Spitschan, M., Jain, S., Brainard, D. H., & Aguirre, G. K. (2014). Opponent melanopsin and S-cone signals in the human pupillary light response. *Proceedings of the National Academy of Sciences of the United States of America*, *111*(43), 15568–15572. https://doi.org/10.1073/pnas.1400942111

Spitschan, M., & Woelders, T. (2018). The method of silent substitution for examining melanopsin contributions to pupil control. *Frontiers in Neurology*, *9*(NOV). https://doi.org/10.3389/fneur.2018.00941

Stefani, O., Bues, M., Pross, A., Mebben, S., Westner, P., Dudel, H., & Rudolph, H. (2012). Moving clouds on a virtual sky affect well-being and subjective tiredness positively. *Proceedings of CIE Lighting Quality and Energy Efficiency*, 19–21.

Stiles, W. S., & Burch, J. M. (1959). N.P.L. Colour-matching investigation: Final report (1958). *Optica Acta: International Journal of Optics*, *6*(1), 1–26. https://doi.org/10.1080/713826267

Stockman, A., MacLeod, D. I. A., & Johnson, N. E. (1993). Spectral sensitivities of the human cones. *Journal of the Optical Society of America A*, *10*(12), 2491. https://doi.org/10.1364/josaa.10.002491

Stockman, A., & Sharpe, L. T. (2000). The spectral sensitivities of the middle- and long-wavelength-sensitive cones derived from measurements in observers of known genotype. *Vision Research*, *40*(13), 1711–1737. https://doi.org/10.1016/S0042-6989(00)00021-3

Stockman, A., Sharpe, L. T., & Fach, C. (1999). The spectral sensitivity of the human short-wavelength sensitive cones derived from thresholds and color matches. *Vision Research*, *39*(17), 2901–2927. https://doi.org/10.1016/S0042-6989(98)00225-9

Trieschmann, M., Van Kuijk, F. J. G. M., Alexander, R., Hermans, P., Luthert, P., Bird, A. C., & Pauleikhoff, D. (2008). Macular pigment in the human retina: histological evaluation

of localization and distribution. *Eye*, *22*(1), 132-137.

https://doi.org/10.1038/sj.eye.6702780

Uprety, S., Adhikari, P., Feigl, B., & Zele, A. J. (2022). Melanopsin photoreception differentially modulates rod-mediated and cone-mediated human temporal vision. *Iscience*, *25*(7), 104529. https://doi.org/10.1016/j.isci.2022.104529

Usui, T., Kremers, J., Sharpe, L. T., & Zrenner, E. (1998). Flicker cone electroretinogram in dichromats and trichromats. *Vision Research*, *38*, 3391–3396.

Vincent, J., Haggerty, E. B., Brainard, D. H., & Aguirre, G. K. (2021). Melanopic stimulation does not alter psychophysical threshold sensitivity for luminance flicker. *Scientific reports*, *11*(1), 20167. https://doi.org/10.1038/s41598-021-99684-0

Virtanen, P., Gommers, R., Oliphant, T. E., Haberland, M., Reddy, T., Cournapeau, D., Burovski, E., Peterson, P., Weckesser, W., Bright, J., van der Walt, S. J., Brett, M., Wilson, J., Millman, K. J., Mayorov, N., Nelson, A. R. J., Jones, E., Kern, R., Larson, E., … Vázquez-Baeza, Y. (2020). SciPy 1.0: fundamental algorithms for scientific computing in Python. *Nature Methods*, *17*(3), 261–272. https://doi.org/10.1038/s41592-019-0686-2

Vos, J. J., & Walraven, P. L. (1970). On the derivation of the foveal receptor primaries. *Vision Research*, *11*(2), 799–818.

Weale, R. A. (1988). Age and the transmittance of the human crystalline lens. *The Journal of Physiology*, *395*(1), 577–587. https://doi.org/10.1113/jphysiol.1988.sp016935

Whitehead, A. J., Mares, J. A., & Danis, R. P. (2006). Macular pigment: A review of current knowledge. *JAMA Ophthalmology*, *124*(7), 1038–1045. https://doi.org/10.1001/archopht.124.7.1038

Wise, E. N., Foster, M. L., Kremers, J., & Mowat, F. M. (2021). A modified silent substitution electroretinography protocol to separate photoreceptor subclass function in lightly sedated dogs. *Veterinary Ophthalmology*, *24*(1), 103–107. https://doi.org/10.1111/vop.12847

Yamakawa, M., Tsujimura, S. I., & Okajima, K. (2019). A quantitative analysis of the

contribution of melanopsin to brightness perception. *Scientific reports*, *9*(1), 7568.

https://doi.org/10.1038/s41598-019-44035-3

Zandi, B., Stefani, O., Herzog, A., Schlangen, L. J., Trinh, Q. V., & Khanh, T. Q. (2021).

Optimising metameric spectra for integrative lighting to modulate the circadian system

without affecting visual appearance. *Scientific reports*, *11*(1), 23188.

https://doi.org/10.1038/s41598-021-02136-y